Numerical and Experimental Study of a Homogenizer Impinging Jet

Andrew R. Kleinig and Anton P. J. Middelberg
Cooperative Research Centre for Tissue Growth and Repair, Dept. of Chemical Engineering, The University of Adelaide, Australia 5005

High-pressure homogenization is a key unit operation used to disrupt cells containing intracellular bioproducts. Modeling and optimization of this unit are restrained by a lack of information on the flow conditions within a homogenizer valve. A numerical investigation of the impinging radial jet within a homogenizer valve is presented. Results for a laminar and turbulent ($k-\epsilon$ turbulent model) jet are obtained using the PHOENICS finite-volume code. Experimental measurement of the stagnation region width and correlation of the cell disruption efficiency with jet stagnation pressure both indicate that the impinging jet in the homogenizer system examined is likely to be laminar under normal operating conditions. Correlation of disruption data with laminar stagnation pressure provides a better description of experimental variability than existing correlations using total pressure drop or the grouping $1/Y^2h^2$.

Introduction

The recovery of intracellular biotechnology products (e.g., vaccines in yeast, proteins in bacteria) relies on a cell-disruption process to release the product from the host microorganism. Of the methods available for process-scale disruption, high-pressure homogenization (a mechanical disruption technique) is the most widely used (Middelberg, 1995) and is the subject of this study.

Essentially, a high-pressure homogenizer consists of a positive displacement pump that forces a suspension through a valve assembly at high pressure. High-pressure homogenizers were first produced approximately 100 years ago for dairy industry applications, and have since been adapted to operate at higher pressures for cell-disruption applications.

This article reviews the physical mechanisms that have been proposed to effect cell disruption during homogenization, and highlights the need for further information relating to homogenizer fluid mechanics. Numerical simulations were then conducted to compare the flow fields within the homogenizer's impinging jet region for laminar and turbulent cases. Experimental measurement of the impinging jet stagnation region width and correlation of cell-disruption efficiency with stagnation pressure were then used to show that the homogenizer's impinging jet is likely to be laminar under normal operating conditions.

Correspondence concerning this article should be addressed to A. P. J. Middelberg.

Previous homogenizer studies

The APV-Gaulin 15MR-8TBA high-pressure homogenizer used in this and many other studies consists of a high-pressure positive-displacement piston pump that forces a cell suspension through a valve unit. As shown in Figure 1, the suspension is fed axially into the valve seat, and then accelerated radially into a small gap between the valve and seat. Once this suspension leaves the gap, it becomes a radial jet that stagnates on an impact ring before leaving the homogenizer at atmospheric pressure. Operating pressure is controlled by adjusting the distance between the valve and seat (h), using a spring-loaded valve.

Experimental studies have shown that the major variables influencing homogenizer performance include homogenizer operating pressure, valve design, number of homogenizer passes, and culture history (Hetherington et al., 1971; Engler and Robinson, 1981; Keshavarz-Moore et al., 1990; Middelberg et al., 1992b). Cell-disruption efficiency is widely modeled using Eq. 1,

$$\ln\left(\frac{1}{1-R}\right) = k_1 N^{k_2} P^{k_3}, \tag{1}$$

with the empirical constants k_1–k_3 dependent on valve design and culture history (Hetherington et al., 1971; Sauer et al., 1989; Keshavarz-Moore et al., 1990; Harrison et al., 1991).

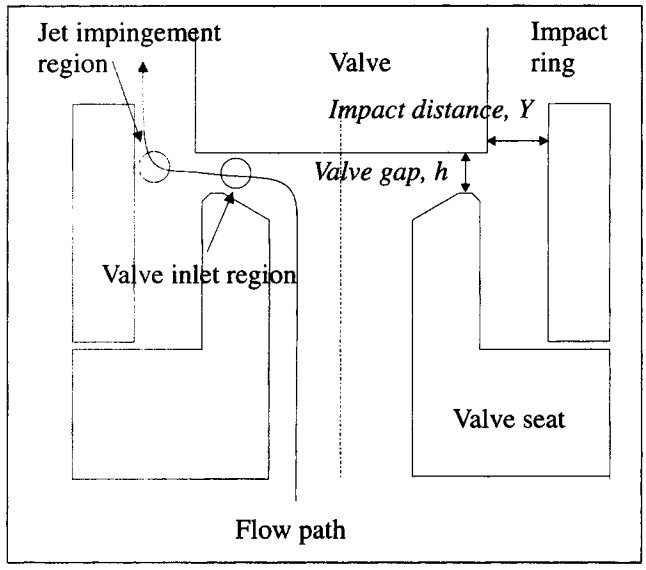

Figure 1. Homogenizer valve assembly.

Equation 1 does not imply the physical processes effecting cell disruption during homogenization.

Middelberg (1995) reviewed the proposed physical processes responsible for the disruption of fat globules and microorganisms during homogenization. For microorganisms, proposed processes include the rate and magnitude of pressure drop (Brookman, 1975; Kelemen and Sharpe, 1979), turbulence (Doulah et al., 1975) and cavitation (Save et al., 1994). Of particular importance are studies conducted by Engler (1980) to independently evaluate the effects of shear, normal, and impingement stresses on cell-disruption efficiency using purpose-built equipment. Impingement was found to be more effective than normal and shear stresses for the disruption of a yeast (Engler and Robinson, 1981). It was also shown that cell disruption during impingement could be correlated with the maximum stagnation pressure of the impinging jet (Eq. 2):

$$P_S = \frac{1}{2}\rho U^2. \tag{2}$$

Keshavarz-Moore et al. (1990) have since confirmed that suspension impingement is important for yeast disruption in an APV-Gaulin homogenizer. Disruption efficiency increased as valve gap and impact distance decreased. Using correlations developed for an impinging turbulent jet (Beltaos and Rajaratnam, 1974), an expression was developed to relate stagnation pressure (and hence disruption rate) to valve gap and impact distance (Eq. 3):

$$P_S \propto \frac{1}{Y^2 h^2}. \tag{3}$$

Equation 3 was verified for a range of valve seat designs and impact distances at a fixed homogenizer operating pressure. For Baker's yeast cells under normal operating conditions, it was found that 80% of cell disruption occurs in the impinging jet, with the remainder occurring in the valve inlet region. Further studies have confirmed the effect of impact distance on disruption efficiency for yeast (Kleinig and Middelberg, 1994), but show that while impact distance is still important for *E. coli* disruption, it is less significant than during yeast disruption (Kleinig et al., 1996).

Although it is apparent that cell disruption is effected by the impinging homogenizer jet, it is difficult to determine the real cause of cell damage during the impingement process. Cell damage may occur as a result of two types of mechanical stress: contact stress and stress related to fluid movement (Engler, 1980; Bavouzet et al., 1995). Different studies have postulated which of these stresses are likely to result in cell disruption. Contact stresses may result from abrasion of cells as they collide with one another (Engler, 1980) or with the stationary impact ring (Middelberg et al., 1992a). Fluid stresses are related to pressure changes (Brookman, 1975; Bavouzet et al., 1995) or viscous shearing stresses (Keshavarz-Moore et al., 1990; Ayazi Shamlou et al., 1995).

To determine which stresses cause cell disruption, knowledge of both destructive stresses generated during homogenization and the physical strength of cells is required (Middelberg et al., 1992a; Ayazi Shamlou et al., 1995). Developments in micromanipulation techniques have allowed the measurement of the strength of mammalian cells (Zhang et al., 1991) and, more recently, yeast cells (Roberts et al., 1994; Srinorakutara et al., 1995). However, the hydrodynamic phenomena occurring in a homogenizer valve have been suggested to be too complicated to allow a straightforward analysis (Engler and Robinson, 1981). Qualitative analysis of flow in a homogenizer valve has been conducted (Ayazi Shamlou et al., 1995). Due to various uncertainties in such a qualitative analysis, destructive stresses can only be estimated approximately.

In this study, we do not attempt to debate the exact nature of the stresses causing cell damage, but examine the fluid flow within the impinging jet region of a homogenizer valve. No studies of flow in this region of a homogenizer valve have been previously reported. This fluid-flow information will be used in future work to provide further insight into the exact nature of the stresses causing cell breakage.

Flow Geometry of Jet Impingement Region

Figure 1 is a diagram of the homogenizer valve assembly. As the cell suspension emerges from the ring-shaped gap formed by the outer edges of the homogenizer valve and seat, a radial fan jet is produced. There is no reported evidence to suggest whether this radial homogenizer jet is laminar or turbulent. Rajaratnam (1976) states that the radial fluid flow obtained from two closely spaced parallel disks into a stagnant environment rapidly becomes turbulent, without giving further qualification. Keshavarz-Moore et al. (1990) assumed the radial homogenizer jet to be turbulent. Turbulent radial jets have been studied experimentally (Heskestad, 1966; Witze and Dwyer, 1976; Tanaka and Tanaka, 1976; Patel, 1979) and numerically (Wood and Chen, 1985; Malin, 1989). The radial jet attains self-similarity after a certain development region, when the velocity half-width increases linearly with distance, and the maximum jet velocity on the symmetry plane decays with distance.

A study of small, impinging circular water jets found jets to be laminar for hydraulic Reynolds numbers of less than 6,000

(Elison and Webb, 1994). As the jet in this homogenizer has a Reynolds number of less than 6,000 (based on $Q = 4.6 \times 10^{-5}$ $m^3 s^{-1}$, $r_e = 0.0045$ m, $\nu = 10^{-6}$ $m^2 s^{-1}$, $Re = Q/\pi r_e \nu = 3{,}200$), it is probable that it is laminar. Laminar radial jets have been examined theoretically (Squire, 1955; Schwarz, 1963) and numerically (Laschefski et al., 1994). At higher Reynolds numbers, a laminar jet has a lower velocity decay rate than the corresponding turbulent jet (Deshpande and Vaishnav, 1982; Elison and Webb, 1994).

It is the jet stagnation point that is of interest for cell disruption (Engler and Robinson, 1981). To our knowledge, no studies have been reported for jet impingement with the same geometry as a high-pressure homogenizer (radial jet impinging on a surface perpendicular to the jet's plane of symmetry). However, impinging jet flows of different geometry occur in a wide variety of situations of practical interest and have been examined. Experimental measurement of velocities and pressures in the turbulent plane and circular impinging jets have been published (Beltaos and Rajaratnam, 1973, 1974). Numerical studies of stagnating turbulent (Champion and Libby, 1994) and laminar (Deshpande and Vaishnav, 1982; Law and Masllyah, 1984) axisymmetric jets have also been reported.

Due to the small size of a homogenizer valve, and the high pressures and velocities of the fluid within the valve, it is likely that large local pressure and velocity gradients exist. To obtain accurate experimental measurements of, for example, stagnation region pressure profiles, extremely small pressure tappings would be required. It is not likely to be possible to produce pressure tappings small enough to obtain accurate measurements. To obtain estimates of stagnation pressure at the homogenizer impact ring, numerical studies are required.

Numerical Simulation

The homogenizer radial jet exits the gap between the valve and valve seat. Initially, a radial wall jet (along the valve face) is formed that becomes a free radial jet as it leaves the valve face. This jet then stagnates at the impact ring. A recirculation zone will exist in the annular space bounded by the jet, valve seat, and impact ring. Fluid exits the valve assembly by passing through the annular gap between the valve and impact ring. To simplify this flow geometry, the radial jet was approximated as a plane-symmetric radial jet (neglecting effects of the recirculation zone), starting at a radial coordinate that is the average of the valve radius and valve-seat exit radius (neglecting the effects of the radial wall jet). The resulting two-dimensional computational domain is shown in Figure 2. Based on experimental measurements of valve gap (Kleinig and Middelberg, 1996), the jet was simulated for valve gaps of 8 to 24 μm.

The fluid was assumed to be steady, Newtonian, isothermal, incompressible, and homogeneous, with constant density and viscosity throughout the domain. The assumption of isothermal and hence constant density and viscosity is only an approximation. A significant temperature rise ($0.22°C \cdot MPa^{-1}$) occurs over the homogenizer. At high operating pressure, this temperature rise will significantly affect fluid viscosity and laminar jet stagnation pressure. However, we estimate that most of this temperature increase occurs after the stagnation point where pressure and kinetic energy are converted to thermal energy. Thus, while an error is introduced by assuming isothermal conditions, it is expected to be less than 10% at the highest operating pressures and does not change the conclusions of this study. Gravity effects were considered negligible and were not included in the calculations. The general transport equations for the resulting fluid flow can be represented by Eq. 4:

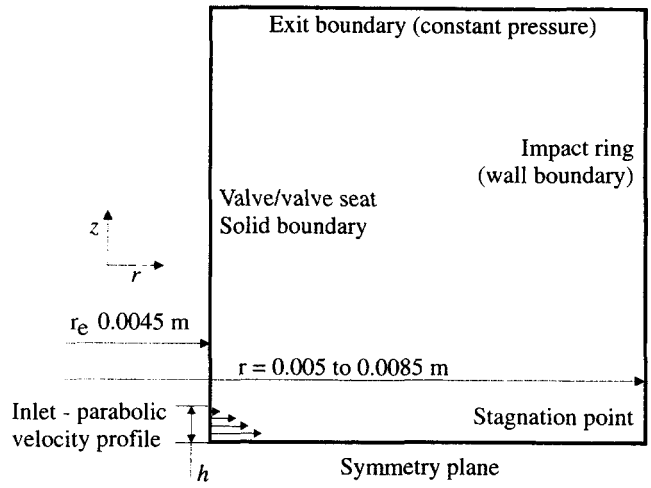

Figure 2. Computational domain used for the jet-impingement region.

$$\text{div}(\rho\phi U) = \text{div}(\Gamma_\phi \text{ grad } \phi) + S_\phi. \quad (4)$$

In Eq. 4, the terms (from left to right) represent convection, diffusion, and source terms. The Navier–Stokes equations can be written in the generalized form of Eq. 4 using the coefficients provided in Table 1. Writing transport equations in the form of Eq. 4 facilitates implementation of a finite-volume numerical solution algorithm.

For calculations involving the case of a laminar jet flow, three equations (continuity, axial momentum, and radial momentum) were solved for pressure, axial velocity, and radial velocity. The PHOENICS 2.1 finite-volume code (CHAM, Wimbledon, London, UK) was used to solve the integrated form of the balance equations.

Calculations were also conducted for the case of a turbulent jet. Turbulence modeling was conducted by using the high Reynolds number Harlow and Nakayama (1968) form of the $k-\epsilon$ turbulence model built into the PHOENICS code. The $k-\epsilon$ turbulence model determines the Reynolds stresses through the use of the Boussinesq eddy viscosity concept, as represented by Eq. 5

Table 1. Coefficients for the Navier–Stokes and k-ϵ Model Transport Equations Written in the Form of Eq. 4

Equation	ϕ	Γ_ϕ	S_ϕ
Continuity	1	0	0 + boundary sources
Radial momentum	V	$\rho(\nu_L + \nu_T)$	−grad(P) + friction
Axial momentum	W	$\rho(\nu_L + \nu_T)$	−grad(P) + friction
Turbulent kinetic energy	k	μ_T/σ_k	$\rho(P_k - \epsilon)$
Turbulent kinetic energy dissipation	ϵ	μ_T/σ_ϵ	$\rho(\epsilon/k)(C_{1\epsilon}P_k - C_{2\epsilon}\epsilon)$

$$-\rho\overline{u_i'u_j'} = \rho\nu_T\left(\frac{\partial U_i}{\partial x_j}+\frac{\partial U_j}{\partial x_i}\right)-\frac{2}{3}\rho k\delta_{ij}, \quad (5)$$

where the eddy viscosity, ν_T, is found from

$$\nu_T = C_\mu\frac{k^2}{\epsilon}. \quad (6)$$

Use of the $k-\epsilon$ model requires the solution of balance equations for k and ϵ (Table 1) in addition to the three equations solved for laminar flow. The volumetric production rate of turbulent kinetic energy (in Table 1) is given by

$$P_k = -\overline{u_i'u_j'}\frac{\partial U_i}{\partial x_j}. \quad (7)$$

This quantity represents the conversion of mean flow kinetic energy into turbulent kinetic energy. Standard values for the five empirical constants in the $k-\epsilon$ model were used and are given in Table 2.

Jet inlet mass flow was fixed to the average homogenizer flow rate of 4.6×10^{-5} m^3s^{-1} (flow rate of 55 L/h, valve open one-third of the time) provided by the homogenizer's positive displacement pump. This flow rate is independent of homogenizer operating pressure to within $\pm2\%$ over the range of operating pressures used. The length of the valve gap is 20–50 times larger than the valve gap itself, which develops a velocity profile that is adequately represented by the parabolic velocity profile given by Eq. 8 (Kleinig and Middelberg, 1996):

$$V = \frac{3Q}{4\pi r_e h}\left[1-\left(\frac{2z}{h}\right)^2\right]. \quad (8)$$

Inlet values of k and ϵ were set by assuming a nominal turbulence intensity of 3% for the inlet flow in the case of a turbulent jet. Although 3% was chosen arbitrarily, the results obtained were insensitive to the actual value used. This is because the radial jet distance is much larger than the initial jet width (> 40 times), and the initial turbulence intensity is rapidly balanced by shear production and dissipation of turbulent kinetic energy within the jet. The flow exit boundary (between the valve and impact ring) was given a fixed pressure boundary condition. The symmetry plane of the radial jet was a symmetry boundary. Solid walls (the valve/valve seat and impact ring) had velocity components fixed to zero at the wall.

The computational domain was divided into 59 axial grid cells and 45 to 85 radial grid cells (depending on the distance to the impact ring). The grid was clustered to give greatest grid refinement at the jet stagnation point. Solutions were also checked for grid independence for a typical case by doubling the number of grid cells in the radial and axial directions. Maximum stagnation pressure was found to differ by less than 1% for the two cases.

Table 2. Values of the Constants Used in the $k-\epsilon$ Turbulence Model

Constant	Value
C_μ	0.09
$C_{1\epsilon}$	1.44
$C_{2\epsilon}$	1.92
σ_k	1.0
σ_ϵ	1.314

Source: Harlow and Nakayama (1968).

Experimental

Radial homogenizer jet width

Due to the small size of the impinging jet, it is not possible to obtain a direct measure of, for example, flow velocities or stagnation pressure profiles. This study does, however, provide a measurement of the jet stagnation region width.

To measure the impinging jet width, the homogenizer was extensively modified. An impact ring was produced that contained a 150-μm radial bleeding hole. This modified impact ring was threaded (1 mm pitch thread) to allow axial movement of the bleeding hole, using an adjusting nut. The modified impact ring and adjusting nut were housed in a two-part valve body, which also housed the valve and valve seat. This arrangement allowed accurate axial positioning of the bleeding hole in the impact ring, and is shown in Figure 3. This experimental arrangement is not able to give quantitative information on the actual stagnation pressure at the bleeding hole, as the bleeding hole is large compared to the dimensions of the stagnation region. The measured stagnation pressure is therefore averaged over a large area. However, axial movement of the bleeding hole provided an estimate of the width of the stagnation region at the impact ring. This was determined by the presence or absence of a jet issuing from the bleeding hole as the hole was translated axially.

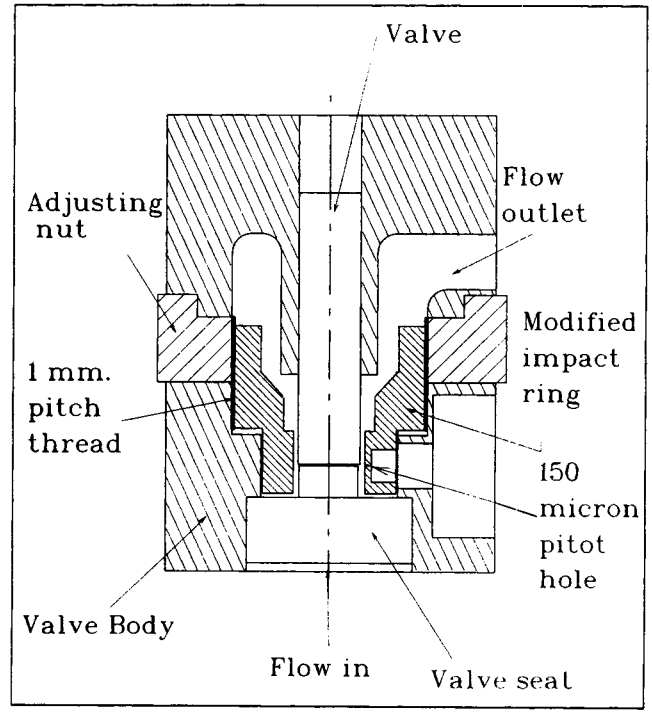

Figure 3. Experimental arrangement used to measure jet width at stagnation.

Results and Discussion

As noted previously, calculations were conducted for the case of both a laminar and turbulent impinging jet. Results obtained for each case are compared and combined with experimental evidence to suggest that the impinging jet is probably laminar in the homogenizer valve used in this study.

Numerical results for radial jets

Initially, calculations were conducted for free radial jets. The free radial jet's maximum (or center-line) velocity is likely to be of most interest, as it will influence the impinging jet's stagnation pressure and hence cell disruption. Numerical results obtained here can be compared with published analytical or semianalytical results for laminar and turbulent impinging jets.

By substituting the parabolic velocity profile of Eq. 8 into the analytical solution for a free radial jet presented by Schwarz (1963), the laminar radial free jet center-line velocity is obtained as Eq. 9:

$$V_{\max} = \left[\frac{81}{3200}\frac{Q^4}{\nu h^2 r_e^2 \pi^4}\right]^{1/3}\left[r^3 - r_e^3 + \frac{3Qr_e h}{50\pi\nu}\right]^{-1/3}. \quad (9)$$

Similarly, for a turbulent free radial jet, Witze and Dwyer (1976) presented the following semianalytical expression for the free jet's center-line velocity (valid for the case of $r_e \gg h$):

$$V_{\max} = \frac{Q}{2\pi r_e h}\left[\frac{1.32 r_e h}{mr(r-r_e)}\right]^{1/2}. \quad (10)$$

Experimentally determined spreading rates (parameter m in Eq. 10) range from 0.098 to 0.110, while the standard $k-\epsilon$ model predicts a spreading rate of 0.090, which is somewhat lower (Malin, 1989). Center-line jet velocity values from Eqs. 9 and 10 are compared with numerical results in Figure 4.

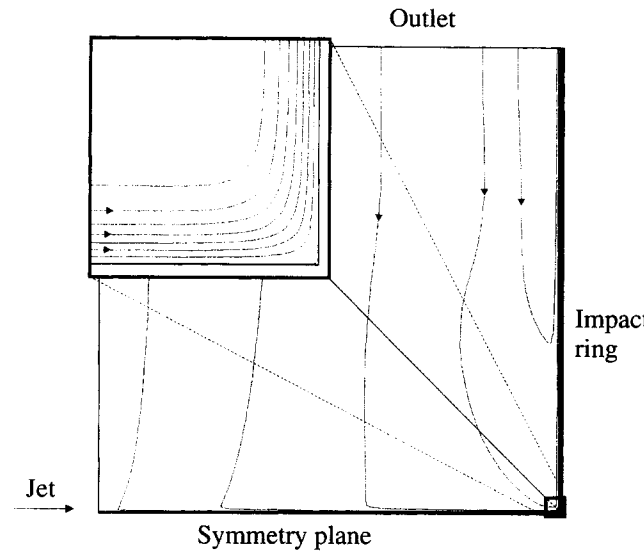

Figure 5. Streamlines in the impinging jet region for a laminar impinging jet.

It is apparent from Figure 4 that the turbulent jet has a considerably more rapid rate of velocity decay with radius than the corresponding laminar jet. Also, the numerical results are in close agreement with available analytical and semianalytical solutions for radial free jets.

Subsequently, numerical results were obtained for impinging jets. For the case of an 8-μm valve gap, and the standard impact ring ($r = 5.5$ mm), laminar and turbulent impinging jet streamlines are compared in Figures 5 and 6, respectively. Due to the lower spreading rate of the laminar jet in comparison with the turbulent jet, the laminar impinging jet has a very small stagnation region. This is seen more clearly by

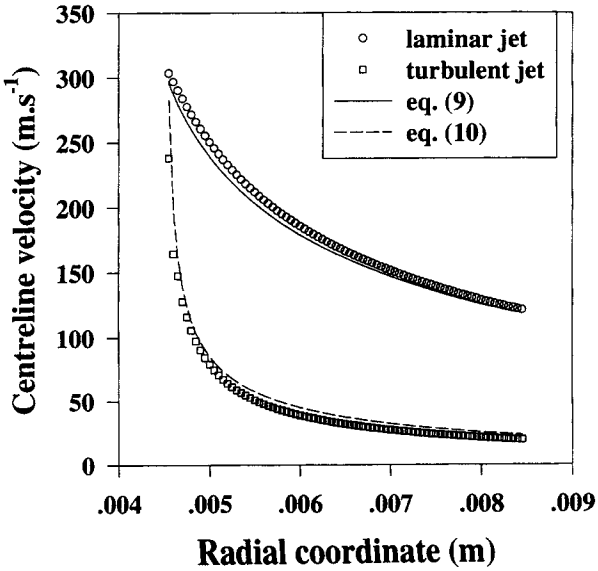

Figure 4. Calculated laminar vs. turbulent free jet axial center-line velocity profile for an 8-μm valve gap.

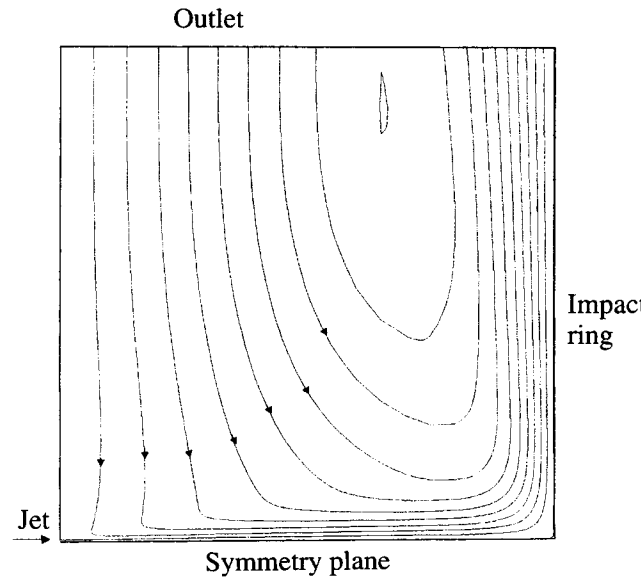

Figure 6. Streamlines in the impinging jet region for a turbulent impinging jet (k-ϵ turbulent model).

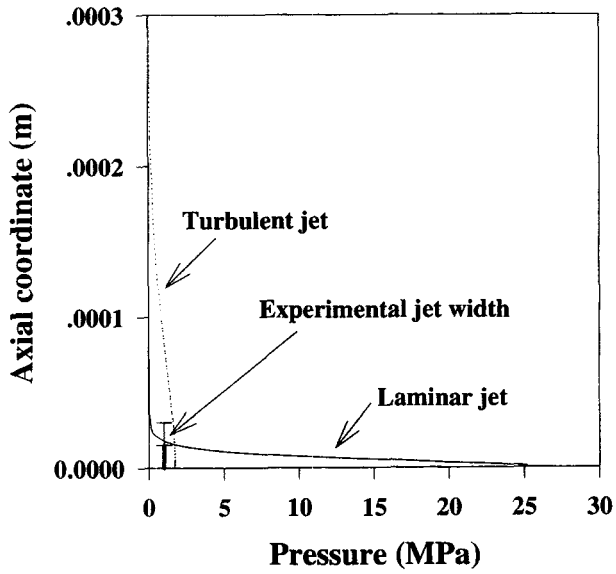

Figure 7. Calculated laminar vs. turbulent jet axial stagnation pressure profile at the jet stagnation point, for an 11.0-mm-dia. impact ring and an 8-μm valve gap.

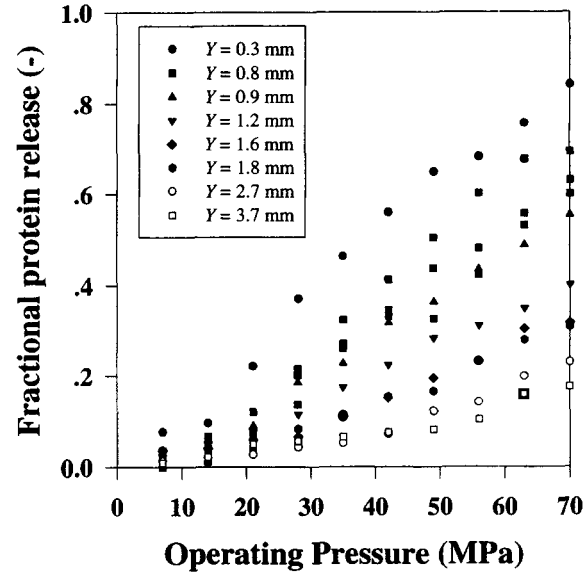

Figure 8. Dependence of baker's yeast disruption on homogenizer operating pressure for a range of impact distances.

comparing the calculated stagnation pressure profiles for the laminar and turbulent jets (Figure 7). The stagnation pressure of the laminar jet is significantly higher than that for the turbulent jet and focused over a considerably smaller axial distance.

Although these numerical results highlight the large quantitative differences between a laminar and turbulent impinging jet, they do not answer the question of which type of flow occurs in practice. This is determined by measuring the stagnation region width at the impact ring and by correlation of experimental disruption data.

Measured homogenizer jet width

The laminar jet width at stagnation is expected to be approximately 40 μm wide for the standard impact ring and cell-disruption valve at 60 MPa, compared with over 400 μm for the corresponding turbulent jet (Figure 7). Experimentally, the width of the stagnation region was found to be 30 ± 30 μm, a range that includes the expected stagnation width of a laminar jet but is much lower than that expected for a turbulent jet. This stagnation width was obtained when a jet was found to issue from the bleeding hole in the modified impact ring over an axial distance of 180 ± 30 μm. After correcting for the diameter of the bleeding hole, this corresponds to the stagnation region width given earlier. This suggests that the impinging jet in this high-pressure homogenizer is probably laminar under standard operating conditions.

Correlation of cell disruption with stagnation pressure

Cell disruption is usually correlated with homogenizer operating pressure. Cell-disruption data obtained for Baker's yeast (data from Kleinig and Middelberg, 1994) is plotted against operating pressure in Figure 8. These data were obtained for a range of impact distances, giving a wide scatter in the disruption achieved at any given operating pressure. For example, at the rated homogenizer operating pressure of 56 MPa, disruption ranges from 75% with the smallest impact ring to 15% for the largest impact ring examined. Keshavarz-Moore et al. (1990) were able to explain the effect of impact distance and valve gap on disruption rate, for one operating pressure, using stagnation pressure calculated from Eq. 3. Although originally only demonstrated for a single operating pressure, it is assumed that the effect of pressure on cell-disruption rate will be explained in Eq. 3 by the variation of valve gap with operating pressure. Experimental measurements of valve gap with operating pressure (Kleinig and Middelberg, 1996: $h\ (\mu\text{m}) = 37 \times P(\text{MPa})^{-0.35}$) were used to calculate the lefthand side of Eq. 3 for the current study. For the disruption data in Figure 8, obtained for a range of operating pressures and impact distances, the stagnation pressure proportionality calculated from Eq. 3 does not explain the variability in disruption data (Figure 9). This indicates that Eq. 3 is not satisfactory for the correlation of disruption data.

Disruption data were then correlated with numerically determined turbulent jet stagnation pressures; see Figure 10 for the results. Turbulent stagnation pressure does not provide an adequate correlator for cell disruption data.

Disruption data were then correlated with laminar impinging jet stagnation pressure calculated numerically, and are shown in Figure 11. From Figure 11, it appears that laminar stagnation pressure provides a good correlator for cell disruption efficiency. The dependence of fractional protein release on stagnation pressure is described using an empirical function with the form of Eq. 11:

$$R = 1 - \exp\left(-\left[\frac{P_S}{a}\right]^b\right). \tag{11}$$

For the yeast data in Figure 11, the regressed parameters a and b are 20.3 MPa and 2.5, respectively. Most of the vari-

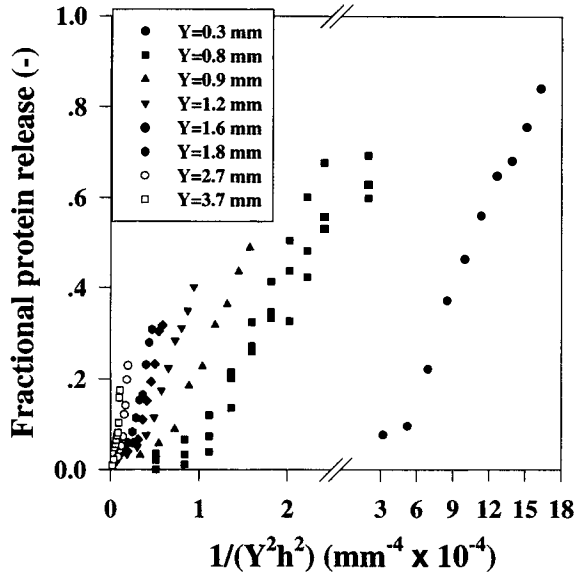

Figure 9. Dependence of baker's yeast disruption on the stagnation pressure proportionality term of Eq. 3 for a range of impact distances.

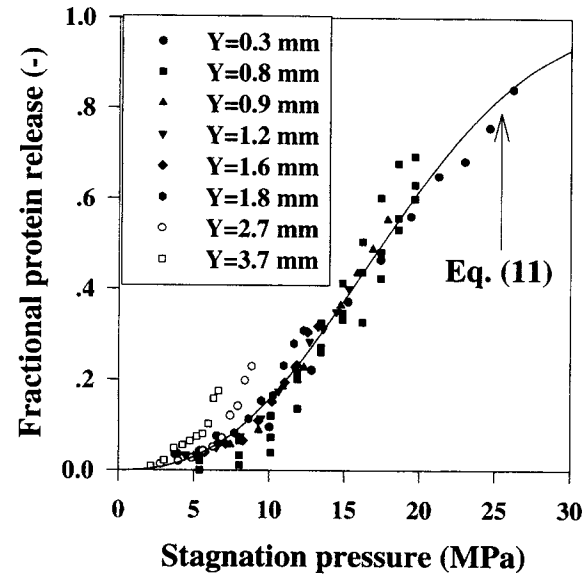

Figure 11. Dependence of baker's yeast disruption on numerically determined laminar jet stagnation pressure for a range of impact distances.

ation in Figure 11 occurs at low values of stagnation pressure. These disruption values correspond to high operating pressures and large impact distances. Under these conditions, it is expected that the cell disruption achieved (< 20%) occurs in the valve inlet region rather than in the stagnation region of the impinging jet, and hence the variation represents the range of disruption that occurs in the valve inlet region before the cells are impinged into the impact ring.

Cell disruption occurs in both the impinging jet and valve inlet regions. It is only in the case of cells where impingement disruption is dominant (for example, yeast cells) that laminar stagnation pressure alone will provide a good correlator for disruption. For cultures where valve inlet disruption is comparable with or greater than impingement disruption under normal operating conditions (for example the *E. coli* data of Kleinig et al. (1996)), laminar stagnation pressure will explain the variation caused by impact distance, but not the initial high level of inlet region disruption. A universally useful model will include terms for disruption that occurs in both the valve inlet and the impingement regions.

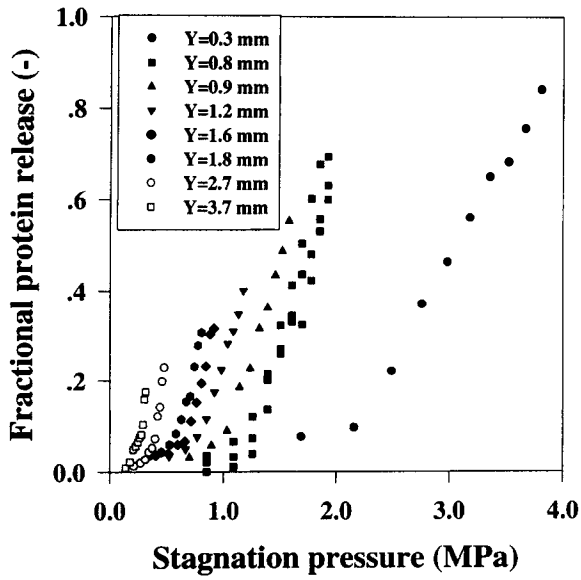

Figure 10. Dependence of baker's yeast disruption on numerically determined turbulent jet stagnation pressure for a range of impact distances.

Conclusions

A numerical study of fluid flow within the impinging jet region of a high-pressure homogenizer was conducted. Results were compared for a laminar and turbulent impinging radial jet. Measurement of stagnation region width, and correlation of cell-disruption efficiency with jet stagnation pressure both indicate that the impinging jet in the homogenizer system examined is likely to be laminar under normal operating conditions. Correlation of disruption data with laminar stagnation pressure provides a better description of experimental variability than existing correlations using total pressure drop or the grouping $1/Y^2h^2$.

Notation

a = empirical constant in Eq. 11, MPa
b = empirical constant in Eq. 11, dimensionless
C = coefficients in the turbulence model
k = turbulent kinetic energy per unit mass, $m^2 \cdot s^{-2}$
m = turbulent jet spreading rate constant, dimensionless
N = number of homogenizer passes
P = pressure, Pa, MPa
P_k = stress production of k, $m^2 \cdot s^{-3}$
Q = flow rate, $m^3 \cdot s^{-1}$
R = fractional cell breakage, dimensionless
r = radial coordinate, m
U = average velocity, $m \cdot s^{-1}$

U = velocity vector
u' = time-varying fluctuating component of instantaneous velocity, $m \cdot s^{-1}$
W = axial velocity, $m \cdot s^{-1}$
Y = homogenizer impact distance (Figure 1), mm
z = axial coordinate, m
δ = Kronecker delta
ϵ = rate of dissipation of k, $m^2 \cdot s^{-3}$
ϕ = general variable (Table 1)
μ = dynamic viscosity, $Pa \cdot s$
ν = kinematic viscosity, $m^2 \cdot s^{-1}$
σ = coefficients in the turbulence model

Subscripts

e = exit
i, j = general coordinates
L = laminar
max = maximum
S = stagnation
T = turbulent
ϕ = variable ϕ

Literature Cited

Ayazi Shamlou, P., S. F. Siddiqi, and N. J. Titchener-Hooker, "A Physical Model of High-Pressure Disruption of Bakers' Yeast Cells," *Chem. Eng. Sci.*, **50**, 1383 (1995).

Bavouzet, J.-M., C. Lafforgue-Delorme, C. Fonade, and G. Goma, "The Effect of an Abrupt Stepwise Reduction in Pressure on the Integrity of the Eukaryotic and Prokaryotic Cell Envelope," *Enzyme Microb. Technol.*, **17**, 712 (1995).

Beltaos, S., and N. Rajaratnam, "Impinging Circular Turbulent Jets," *Proc. ASCE J. Hydraul. Div.*, **100**, 1313 (1974).

Beltaos, S., and N. Rajaratnam, "Plane Turbulent Impinging Jets," *J. Hydraul. Res.*, **11**, 29 (1973).

Brookman, J. S. G., "Further Studies on the Mechanism of Cell Disruption by Extreme Pressure Extrusion," *Biotechnol. Bioeng.*, **17**, 465 (1975).

Champion, M., and P. A. Libby, "Reynolds Stress Description of Opposed and Impinging Turbulent Jets. II. Axisymmetric Jets Impinging on Nearby Walls," *Phys. Fluids*, **6**, 1805 (1994).

Deshpande, M. H., and R. N. Vaishnav, "Submerged Laminar Jet Impingement on a Plane," *J. Fluid Mech.*, **114**, 213 (1982).

Doulah, M. S., T. H. Hammond, and J. S. G. Brookman, "A Hydrodynamic Mechanism for the Disintegration of *Saccharomyces cerevisiae* in an Industrial Homogenizer," *Biotechnol. Bioeng.*, **17**, 845 (1975).

Elison, B., and B. W. Webb, "Local Heat Transfer to Impinging Liquid Jets in the Initially Laminar, Transitional, and Turbulent Regimes," *Int. J. Heat Mass Transfer*, **37**, 1207 (1994).

Engler, C. R., and C. W. Robinson, "Disruption of *Candida utilis* Cells in High Pressure Flow Devices," *Biotechnol. Bioeng.*, **23**, 765 (1981).

Engler, C. R., "Disruption of Microorganisms in High Pressure Flow Devices," PhD Thesis, University of Waterloo, Waterloo, Ont. Canada (1980).

Harlow, F. H., and P. I. Nakayama, "Transport of Turbulence Energy Decay Rate," Los Alamos Science Lab., Univ. of California, Los Alamos, NM (1968).

Harrison, S. T. L., H. A. Chase, and J. S. Dennis, "The Disruption of *Alcaligenes eutrophus* by High Pressure Homogenization: Key Factors Involved in the Process," *Bioseparation*, **2**, 155 (1991).

Heskestad, G., "Hot-Wire Measurements in a Radial Turbulent Jet," *ASME J. Appl. Mech.*, **23**, 31 (1976).

Hetherington, P. J., M. Follows, P. Dunnill, and M. D. Lilly, "Release of Protein from Bakers' Yeast (*Saccharomyces cerevisiae*) by Disruption in an Industrial Homogenizer," *Trans. Inst. Chem. Eng.*, **49**, 142 (1971).

Kelemen, M. V., and J. E. E. Sharpe, "Controlled Cell Disruption: A Comparison of the Forces Required to Disrupt Different Microorganisms," *J. Cell Sci.*, **35**, 431 (1979).

Keshavarz-Moore, E., M. Hoare, and P. Dunnill, "Disruption of Baker's Yeast in a High-Pressure Homogenizer: New Evidence on Mechanism," *Enzyme Microb. Technol.*, **12**, 764 (1990).

Kleinig, A. R., and A. P. J. Middelberg, "The Disruption of Yeasts by High-Pressure Homogenization," *Better Living Through Innovative Biochemical Engineering*, W. K. Teo, M. G. S. Yap, and S. K. W. Oh, eds., *Proc. APBioChEC '94, Third Asia-Pacific Biochemical Engineering Conf.*, Sinapore, p. 607 (1994).

Kleinig, A. R., and A. P. J. Middelberg, "The Correlation of Cell Disruption with Homogenizer Pressure Gradient Determined by Computational Fluid Dynamics," *Chem. Eng. Sci.*, **51**, 5103 (1996).

Kleinig, A. R., B. K. O'Neill, and A. P. J. Middelberg, "The Effect of Homogenizer Impact Distance on the Disruption of *Escherichia coli*," *Biotechnol. Tech.*, **10**, 199 (1996).

Law, H., and J. H. Masllyah, "Mass Transfer Due to Confined Laminar Impinging Axisymmetric Jet," *Ind. Chem. Eng. Fundam.*, **23**, 446 (1984).

Laschefski, H., D. Braess, H. Haneke, and N. K. Mitra, "Numerical Investigations of Radial Jet Reattachment Flows," *Int. J. Numer. Methods Fluids.*, **18**, 629 (1994).

Malin, M. R., "Modeling the Effects of Lateral Divergence on Radially Spreading Turbulent Jets," *Comput. Fluids*, **17**, 453 (1989).

Middelberg, A. P. J., "Process-Scale Disruption of Microorganisms," *Biotechnol. Adv.*, **13**(3), 491 (1995).

Middelberg, A. P. J., B. K. O'Neill, and I. D. L. Bogle, "A New Model for the Disruption of *Escherichia coli* by High-Pressure Homogenization. I. Model Development and Verification," *Trans. Inst. Chem. Eng.*, **70**(C), 205 (1992a).

Middelberg, A. P. J., B. K. O'Neill, I. D. L. Bogle, N. J. Gully, A. H. Rogers, and C. J. Thomas, "A New Model for the Disruption of *Escherichia coli* by High-Pressure Homogenization. II. A Correlation for the Effective Cell Strength," *Trans. Inst. Chem. Eng.*, **70**(C), 213 (1992b).

Patel, R. P., "Some Measurements in Radial Free Jets," *AIAA J.*, **17**, 657 (1979).

Rajaratnam, N., "The Radial Jet," *Turbulent Jets*, Elsevier, New York, p. 50 (1976).

Roberts, A. D., Z. Zhang, T. W. Young, and C. R. Thomas, "Direct Determination of the Strength of Brewing Yeast Cells Using Micromanipulation," *Proc. Ind. Chem. Eng. Ann. Res. Event*, University College, London, p. 73 (1994).

Sauer, T., C. W. Robinson, and B. R. Glick, "Disruption of Native and Recombinant *Escherichia coli* in a High-Pressure Homogenizer," *Biotechnol. Bioeng.*, **33**, 1330 (1989).

Save, S. S., A. B. Pandit, and J. B. Joshi, "Microbial Cell Disruption: Role of Cavitation," *Chem. Eng. J.*, **55**, B67 (1994).

Schwarz, W. H., "The Radial Free Jet," *Chem. Eng. Sci.*, **18**, 50 (1963).

Squire, H. B., "Radial Jets," *50 Jahre Grenzschichtforschung*, Vieweg, Braunschweig, FRG, p. 47 (1955).

Srinorakutara, T., Z. Zhang, and C. R. Thomas, "Mechanical Properties of Yeast," *CHEMECA '95, Proc. Australasian Chemical Engineering Conf.*, Adelaide, Australia, Vol. 3, p. 45 (1995).

Tanaka, T., and E. Tanaka, "Experimental Investigation of a Radial Turbulent Jet," *Bull. JSME*, **19**, 792 (1976).

Witze, P. O., and H. A. Dwyer, "The Turbulent Radial Jet," *J. Fluid Mech.*, **75**, 401 (1976).

Wood, P. E., and C. P. Chen, "Turbulence Model Predictions of the Radial Jet—A Comparison of $k - \epsilon$ Models," *Can. J. Chem. Eng.*, **63**, 177 (1985).

Zhang, Z., M. A. Ferenczi, A. C. Lush, and C. R. Thomas, "A Novel Micromanipulation Technique for Measuring the Bursting Strength of Single Mammalian Cells," *Appl. Microbiol. Biotechnol.*, **36**, 208 (1991).

Manuscript received Aug. 7, 1996, and revision received Nov. 7, 1996.